

Experimental search for the electrical spin injection in a semiconductor

A. T. Filip, B. H. Hoving, F. J. Jedema, and B. J. van Wees

Department of Applied Physics, University of Groningen, Groningen 9747AG, The Netherlands

B. Dutta and S. Borghs

IMEC, Kapeldreef 27, Leuven, Belgium

(Received 6 June 2000)

The electrical injection of spin-polarized electrons in a semiconductor can be achieved in principle by driving a current from a ferromagnetic metal, where current is known to be significantly spin polarized, into the semiconductor via Ohmic conduction. For detection a second ferromagnet can be used as a drain. We studied submicron lateral spin valve junctions, based on high-mobility InAs/AlSb two-dimensional electron gas, with Ni, Co, and permalloy as ferromagnetic electrodes. In the standard geometry it is very difficult to separate true spin injection from other effects, including local Hall effect, anomalous magnetoresistance contribution from the ferromagnetic electrodes and weak localization/antilocalization corrections, which can closely mimic the signal expected from spin valve effect. The reduction in size, and the use of a multiterminal nonlocal geometry allowed us to reduce the unwanted effects to a minimum. Despite all our efforts, we have not been able to observe spin injection. However, we find that this “negative” result in these systems is actually consistent with theoretical predictions for spin transport in diffusive systems.

The idea to use the spin of the electron in electronic devices has gained a lot of momentum lately, leading to the appearance of the field of “spintronics.”¹ It is envisioned that spin sensitive electronics would open new perspectives to semiconductor device technology. The potential to inject and control the electronic spin in a semiconducting material is also of great interest for the field of quantum computation.² The first active device was suggested a decade ago by Datta and Das,³ who proposed an electronic device analogous to the electro-optic modulator. The essential requirements for such a device is the efficiency of injection of the spin-polarized carriers into the semiconductor and the long spin relaxation time. The latter requirement was shown to be met in time resolved optical experiments at low temperatures, where lifetimes as long as $0.1 \mu\text{s}$ for spin in GaAs were observed.⁴ Regarding the issue of spin injection, different approaches were taken. Optical injection and detection of spin polarized carriers in semiconductors have been shown in a experiment by J. Kikkawa and D. D. Awschalom.⁵ Spin injection from a ferromagnetic Scanning tunnel microscope tip into GaAs has also been demonstrated.⁶ The electrical injection from a fully polarized magnetic semiconductor, used as spin aligner, into a semiconductor and optical detection, was also shown.⁷

From a device point of view, a major breakthrough would be to have all electronic devices, preferably operating at room temperature. Therefore large efforts have been dedicated to observe the spin valve effect, with semiconductors as the “intermediate” layer.⁸ Recently Hammar *et al.*⁹ have claimed the observation of electrical spin injection in a two-dimensional electron gas (2DEG), by making use of the Rashba spin orbit interaction in the semiconductor heterostructure as the detection mechanism. However, this work has been commented upon and it was suggested that in such a system the detection is not possible within linear transport,¹⁰ and the observed behavior is probably related to

a local Hall effect.¹¹ Gardelis *et al.*¹² claim to have observed spin valve effects in a semiconductor field-effect transistor with Py source and drain. A finite spin polarization of the semiconductor itself was required in order to interpret the experimental observations as spin valve effect. Another interesting approach has been taken by Meier *et al.*,¹³ who tried to observe spin injection by modulating the spin-orbit interaction via an external gate. Hu *et al.*,¹⁴ by measuring in a multi-injector HEMT geometry with ferromagnetic electrodes, observed a gate and electrode spacing difference in the magnetoresistive behavior, which they attributed to spin injection. However, the fact that the standard lateral spin valve geometry leads to important local Hall phenomena has already been pointed out.¹⁵ Due to the dependence on the local magnetization of the contacts, these spurious phenomena will often closely resemble the signals expected from spin transport. In our opinion, none of the previously mentioned experiments give an unambiguous proof of spin dependent transport.

In our experiments, we considered the multiterminal lateral spin valve geometry, as depicted in Fig. 1(b). Two types of measurements are possible. In the first one, called the “classic” spin valve geometry, the current is injected and taken out from the ferromagnetic electrodes. The voltage is measured between the same electrodes, giving a standard four terminal measurement of the junction. A second geometry, which we refer to as the nonlocal geometry, corresponds to injecting current from the semiconducting channel into the first ferromagnetic electrode and measure the voltage between the second ferromagnetic electrode and the semiconducting channel (see Fig. 1). Due to current polarization in the injecting ferromagnet, at the interface a spin accumulation will form, which will extend over a characteristic spatial length scale given by the spin-flip length. If a second ferromagnet is present in the vicinity of this interface, it can be used as a spin sensitive voltage probe to detect this spin

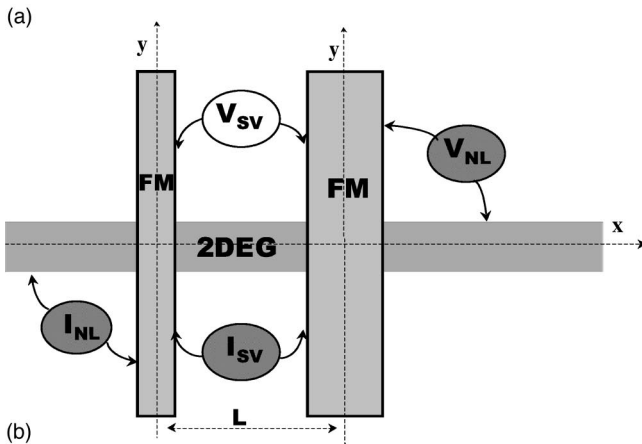
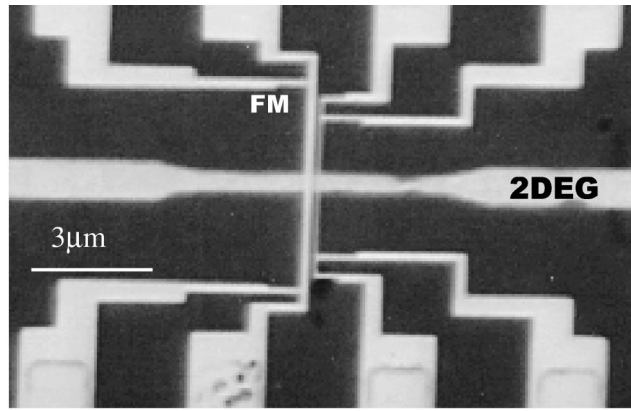


FIG. 1. (a) Scanning electron microscope (SEM) micrograph of a sample. The $1\ \mu\text{m}$ wide 2DEG channel is horizontal, and two ferromagnetic electrodes are vertical. (b) Sketch of the two measurement configurations. The indices “SV” and “NL” refer to the classic spin-valve and, respectively, to the nonlocal geometry. In the latter there is no current flow between injector and detector.

accumulation. This is similar to the Johnson’s potentiometric method,¹⁶ used for detecting spin accumulation in Au. However, the essential advantage of a true lateral geometry resides in the fact that no electrical current is flowing between the injector and the detector electrodes. Therefore this geometry allows to suppress any “spin independent” magnetoresistive contribution, i.e., the weak localization/antilocalization change in conductivity of the semiconductor, and a possible magnetoresistance contribution of the interface resistance.

The experiments were performed on devices made from high mobility InAs/AlSb heterostructures, molecular beam epitaxy grown on an GaAs substrate. Figure 1(a) shows a scanning electron microscope (SEM) image of the FM/2DEG/FM junctions. Prior to processing, the top barrier layer was removed by wet chemical etching with Microposit MF321 photoresist developer. The exposed 15nm thick InAs layer hosts a 2DEG with an electron density $n_s = 1.5 \times 10^{16}\ \text{m}^{-2}$ and a mobility of $\mu = 1.5\ \text{V/m}^2\text{s}$. In the first step, 40nm thick Ti/Au metallization contacts were deposited by means of optical lithography and e -beam evaporation. An approximately $1\ \mu\text{m}$ wide 2DEG channel was defined by optical lithography and selective wet chemical etching, with a succinic acid based solution. The use of wet etching techniques kept the mesa at the smallest height possible, only 15 nm. Consequently, this allowed to reduce the spurious con-

tribution due to local Hall effects at the mesa edges to a minimum. In the last step the ferromagnetic electrodes were defined by means of electron-beam lithography. In order to ensure different coercive fields, the two electrodes had different widths, 150 and 300 nm in case of Py and Co samples, and 150 and 450 nm for the Ni samples. On all samples the electrode lengths were 8 and, respectively, 12 μm , the spacing was 300 nm, and the thickness of the ferromagnetic layer was 60 nm. Co and Py were deposited by sputtering, and Ni by e -beam evaporation. Prior to deposition, the InAs surface was cleaned by means of a low-voltage Ar plasma etching. This was done in order to remove the native InAs oxide and to ensure good Ohmic contact between the semiconductor and the ferromagnet. The cleaning procedure is known to affect the InAs layer by enhancing the electron density and reducing mobility. As a consequence, a diffusive three-dimensional InAs region is formed underneath the ferromagnetic contacts. The square resistances were in the order of 2–4 Ω for the ferromagnets and 300 Ω for the 2DEG channel. The measured interface resistance were around 350 Ω and 750 Ω for the wide and, respectively, the narrow electrode. Based on 2DEG material parameters, by evaluating the number of modes in our channel, we calculated an average ferromagnet/InAs interface transmission in the order of 30%. For comparison, samples where the native InAs surface was left intact were also made. In this case the contact resistance varied between 10 and 100 $\text{k}\Omega$.

Measurements were performed by standard ac-lock-in techniques, both at room temperature and at 4.2 K. The switching behavior of the electrodes was characterized by four terminal anomalous magnetoresistance (AMR) measurements of the ferromagnetic electrodes. In most devices, in contrast to the room-temperature behavior, where a clear difference in the coercive fields of the two electrodes could be established, the exact coercive fields at helium temperature could not be inferred. At 4.2 K the AMR curves in parallel magnetic field showed only a smooth behavior, the switching events being not visible. However, in some of the devices, clear switching of the magnetization direction of each electrode could be observed. Figure 2 shows one representative plot of a Py/2DEG/Py device where the presence of different coercive field for the two electrodes could be established. No resistance modulation is observed when the two ferromagnets switch from a parallel to an antiparallel configuration. We carefully characterized over 20 devices with different ferromagnetic materials, out of which at least three showed switching events in the 4.2 K AMR curves, but no signal that could be attributed to spin injection was observed.

The outstanding question is to what extent can we understand these results. Assuming weak spin scattering, the transport can be described in terms of two independent spin channels. This corresponds to an approach based on the standard Fert-Valet model for describing spin transport.¹⁷ The theoretical implications for a two terminal geometry without spin-flip processes in the semiconductor have already been worked out by Schmidt *et al.*¹⁸ Here we extend the analysis to the multiterminal geometry sketched in Fig. 1, and we also allow for a finite spin-flip length in the semiconductor. The ferromagnets and the semiconductor are treated as diffusive one-dimensional channels. Therefore the transport properties of each channel are fully determined by the bulk conductivi-

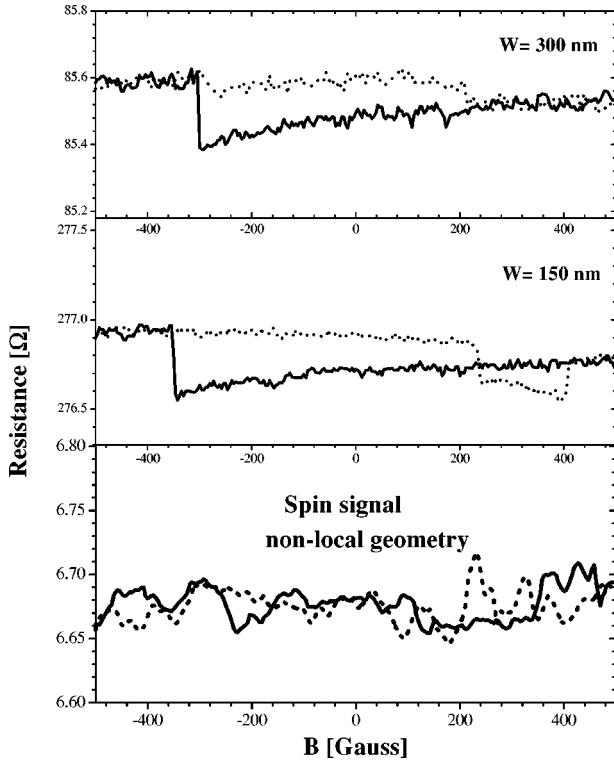


FIG. 2. Spin valve measurements for a Py/2DEG/Py device. Top two curves give the AMR traces for the two ferromagnetic electrodes, showing different coercive fields in one sweep direction. No spin signal is observed in any of the geometries. The dashed lines correspond to a sweep of the magnetic field towards positive fields.

ties (σ_F and, respectively, σ_N), the spin-flip lengths (λ_F and λ_N), and, for the ferromagnet, the bulk spin polarization of the current [$\alpha_F = (\sigma_\uparrow - \sigma_\downarrow) / (\sigma_\uparrow + \sigma_\downarrow)$]. If a current is driven through such a nonhomogeneous system, the electrochemical potential for spin-up and spin-down electrons (μ_\uparrow and μ_\downarrow) can be nonequal. This difference, due to different conductivities in the two spin channels, will decay differently in a ferromagnet than in a normal region, leading to a measurable voltage.

The spin transport, within the relaxation-time approximation, is described by the diffusion equation

$$D \frac{\partial^2 (\mu_\uparrow - \mu_\downarrow)}{\partial x^2} = \frac{(\mu_\uparrow - \mu_\downarrow)}{\tau_{sf}}, \quad (1)$$

where, τ_{sf} is the spin-flip scattering time, and D is the spin averaged diffusion constant [$D = (N_\uparrow + N_\downarrow)(N_\uparrow/D_\uparrow + N_\downarrow/D_\downarrow)^{-1}$, with $N(E_F)$ the density-of-states at the Fermi level]. The currents are related to electrochemical potentials via Ohm's law

$$j_{\uparrow,\downarrow} = - \left(\frac{\sigma_{\uparrow,\downarrow}}{e} \right) \frac{\partial \mu_{\uparrow,\downarrow}}{\partial x}. \quad (2)$$

The charge and spin conservation at each interface has also to be taken into consideration. We assume transparent interfaces, thus we also require the equality of the chemical potential on both sides of the interface.

By adding the appropriate boundary conditions at infinity, so that far away from the interface one recovers the bulk

transport properties, the previous system of equations can be solved analytically for the two geometries depicted in Fig. 1(a).

The resistance change between the parallel and the anti-parallel configuration of the magnetizations of the two electrodes in the ‘‘classic’’ spin valve geometry is given by

$$\Delta R_{SV} = 2R_{sq} \frac{\lambda_N}{w} \frac{\alpha_F^2}{(M^2 + 1) \sinh(L/\lambda_N) + 2M \cosh(L/\lambda_N)} \quad (3)$$

with

$$M = 1 + \frac{\sigma_F \lambda_N}{\sigma_N \lambda_F} (1 - \alpha_F^2).$$

R_{sq} is the square resistance of the semiconductor, L is the spacing between the two ferromagnets, and w is the width of the channel. In the nonlocal configuration the signal is reduced by a factor of 2, $\Delta R_{NL} = \frac{1}{2} \Delta R_{SV}$.

In the limit $\lambda_N \rightarrow +\infty$, one recovers a result similar to the one predicted by Schmidt *et al.* for the standard geometry¹⁸

$$\Delta R_{NL} \approx R_{sq} \frac{\lambda_F^2}{wL} \left(\frac{\sigma_F}{\sigma_N} \right)^2 \frac{\alpha_F^2}{1 - \alpha_F^2}. \quad (4)$$

The relevant range of parameters for ferromagnet/2DEG/ferromagnet junctions is $\sigma_F \gg \sigma_N$ and $\lambda_N \gg \lambda_F$, meaning that, for a spin polarization of the ferromagnet smaller than 100%, the conductivity mismatch correction factor M is large, $M \gg 1$. Then the expected signal can be expressed as

$$\Delta R_{NL} = R_{sq} \frac{\lambda_N}{w} \frac{1}{\sinh(L/\lambda_N)} (\alpha_F/M)^2, \quad (5)$$

i.e., the injection efficiency is reduced from α_F to α_F/M . This shows that the spin valve signal is reduced due to the conductivity mismatch between the semiconductor and the ferromagnet. Moreover, the spin injection efficiency is very sensitive to the spin-flip length in the ferromagnetic material. If this length is small, the expected spin signal is also reduced.

Based on giant magnetoresistance (GMR) experiments,¹⁹ a spin-flip length between 8 and 40 nm and a bulk current spin polarization around 35% is expected for Py. Assuming for the 2DEG a spin-flip length an order of magnitude of 1 μm , we obtain the reduction in spin injection efficiency, $M = 90$. This corresponds to an absolute signal of 0.2 m Ω , or in the order of magnitude of 10^{-6} of the square resistance. The best signal resolution we could obtain was only 5 m Ω , so the expected spin signal was well below the sensitivity threshold.

The direct conclusion to be extracted from the modeling, also pointed out by Schmidt *et al.*,¹⁸ is that the conductivity mismatch blocks spin injection. This result stems from the fact that the lowest conductance in the problem, the conductance of the semiconductor, is spin independent. One possible solution is to make use of magnetic semiconductors, with low conductivity or very high-spin polarization, as in the experiments of Fielderling *et al.* and Ohno *et al.*⁷ A sec-

ond choice would be to use tunnel barriers as the injecting mechanism, where the spin polarization of the tunneling current depends directly on the products of the densities-of-states in the two materials.

One more aspect should also be considered: What is the actual reliability of the model. Recently we were able to observe spin valve effects in a similar geometry with Cu replacing the semiconductor as the normal channel.²⁰ Using the values obtained in GMR experiments for the spin-flip lengths and spin polarization in the ferromagnet,¹⁹ the order of magnitude of the observed effect was in quantitative agreement to the theoretical predictions. Obviously, the main difference in the all metal devices was the absence of conductivity mismatch between the two materials. A potential limitation in the semiconductor case is the fact that the 2DEG channel is quasiballistic. Nevertheless, the presence of the diffusive regions underneath the ferromagnetic contacts should allow us to use a diffusive model to describe spin injection. Moreover, the conductivity mismatch arguments should also be valid for a purely ballistic channel. In that case, the expected signal should be given by an analogous of Eq. (5), with the diffusive 1D conductivity of the semiconductor being replaced by the inverse of the Sharvin

resistance, due to presence of only a few models in the 2DEG channel. Thus the conductivity mismatch arguments should be valid in any device with where the intermediate region has the lowest conductivity, for example, in the case of carbon nanotubes.²¹

In conclusion, submicron lateral spin valve structures in high-mobility InAs/AlSb heterostructures have been fabricated, with Ni Co and Py as ferromagnetic electrodes. Despite all efforts to improve signal resolution and eliminate spurious effects, no spin injection was observed. By no means can this “negative” outcome of our experiments be considered as a proof that spin injection in a semiconductor is not possible with the usual metallic ferromagnets. However, the agreement with theoretical predictions casts some doubt on the feasibility of straightforward spin injection from a metallic ferromagnet into a semiconductor.

This work was supported by the Dutch Foundation for Fundamental Research on Matter (FOM) and European Commission (ESPRIT-MELARI consortium Spider). We acknowledge useful discussions with G. Schmidt and L. Molenkamp. We thank T. M. Klapwijk for his stimulating support in this work.

-
- ¹G.A. Prinz, *Science* **282**, 1660 (1998); B.E. Kane, *Nature (London)* **393**, 133 (1998).
- ²D.P. DiVincenzo, *Science* **269**, 255 (1995).
- ³S. Datta and B. Das, *Appl. Phys. Lett.* **56**, 665 (1990).
- ⁴J. Kikkawa and D.D. Awschalom, *Nature (London)* **397**, 139 (1999).
- ⁵J. Kikkawa and D.D. Awschalom, *Science* **277**, 1284 (1997).
- ⁶S. Alvarado and P. Renaud, *Phys. Rev. Lett.* **68**, 1387 (1999).
- ⁷R. Fielderling, G. Reuscher, W. Ossau, G. Schmidt, A. Waag, and L.W. Molenkamp, *Nature (London)* **282**, 787 (2000); Y. Ohno, D.K. Young, B. Beschoten, F. Matsukara, H. Ohno, and D.D. Awschalom, *ibid.* **282**, 790 (2000).
- ⁸A. Cabbibo *et al.*, *J. Vac. Sci. Technol. A* **15**, 1215 (1997).
- ⁹P.R. Hammar, B.R. Bennet, M.J. Yang, and M. Johnson, *Phys. Rev. Lett.* **83**, 203 (1999).
- ¹⁰B.J. van Wees, *Phys. Rev. Lett.* **84**, 5022 (2000).
- ¹¹F.G. Monzon, H.X. Tang, and M.L. Roukes, *Phys. Rev. Lett.* **84**, 5022 (2000).
- ¹²S. Gardelis, C.G. Smith, C.H. Barnes, E.H. Linfield, and D.A. Ritchie, *Phys. Rev. B* **60**, 7764 (1999).
- ¹³G. Meier *et al.* (preprint).
- ¹⁴C.M. Hu, J. Nitta, A. Jensen, J.B. Hansen, and H. Takayanagi (preprint).
- ¹⁵H.X. Tang, F.G. Monzon, R. Lifshitz, M.C. Cross, and M.L. Roukes, *Phys. Rev. B* **61**, 4437 (2000).
- ¹⁶M. Johnson, *Phys. Rev. Lett.* **70**, 2142 (1993).
- ¹⁷T. Valet and A. Fert, *Phys. Rev. B* **48**, 7099 (1993).
- ¹⁸G. Schmidt, L. Molenkamp, A.T. Filip, and B.J. van Wees, *Phys. Rev. B* **62**, R4790 (2000).
- ¹⁹G. Dubois *et al.*, *Phys. Rev. B* **60**, 477 (1999); P. Holody *et al.*, *ibid.* **58**, 12 230 (1998).
- ²⁰F.J. Jedema, A.T. Filip, and B.J. van Wees, *Nature (London)* (submitted).
- ²¹K. Tsukagoshi, B.W. Alphenaar, and H. Ago, *Nature (London)* **401**, 572 (1999).